ELSEVIER

Catalysis Today 27 (1996) 221–227

CATALYSIS TODAY

Photocatalytic decomposition of chloroform in a fully irradiated heterogeneous photoreactor using titanium oxide particulate suspensions

Carlos A. Martín, Miguel A. Baltanás, Alberto E. Cassano *

INTEC [1] (U.N.L. and CONICET [2]), Güemes 3450, 3000 Santa Fe, Argentina

Abstract

The photocatalytic decomposition of $HCCl_3$ was studied in a fully irradiated photoreactor (FIP) by varying the concentrations of (a) chloroform, (b) dissolved oxygen and (c) titania, as well as (d) the local volumetric rate of energy absorption (LVREA). Fully irradiated conditions are achievable when all the particles along the light path 'see the photons'. In order to compute the VREA (average value of the LVREA), the radiative transfer equation (RTE) was applied to the reactor and solved using a simplified radiation model. Model parameters, i.e., optical properties, as well as the boundary condition for the RTE were obtained experimentally.

Initial rate data of the chloroform decomposition showed that, within the studied range of process variables and under fully irradiated conditions: (1) The reaction rate is of first order with respect to $[HCCl_3]$, zero order with respect to $[O_2]$ and about one-half-order with respect to the LVREA inside the reactor and (2): The effects due to catalyst concentration are fully accounted for within the LVREA dependence.

Keywords: Photocatalytic reactors; Titanium dioxide; Chloroform decomposition

1. Introduction

Worldwide, contemporary urban and industrial developments have boosted the amount of dissolved pollutants, both in surface and underground water streams. In particular, chlorinated hydrocarbons have become a serious environmental threat, since some of them (e.g., chloroform, perchloroethylene) are not just industrial wastes, but also the by-products of the potabilization processes themselves [1]. These ubiquitous compounds share several worrisome qualities, among which carcinogenicity and refractability to conventional clean-up procedures have earned them the Priority Pollutant tag.

In recent years, photocatalytic reactions have received increasing attention, due to their ability to destroy water contaminants [2–4]. Most of that work has been focused on the chemistry and apparent kinetics of the advanced oxidation (mineralization) of many organic substrates using suspensions of powdered semiconductors (notably titanium dioxide) and the mechanisms of the processes involved in these reactions.

Catalysis by illuminated TiO_2 is the result of the interaction of the electrons and holes generated

* Corresponding author.

[1] Instituto de Desarrollo Tecnológico para la Industria Química.

[2] Universidad Nacional del Litoral and Consejo Nacional de Investigaciones Científicas y Técnicas.

SSDI 0920-5861(95)00191-3

in the photoactivated semiconductor with the surrounding medium; thus, as a consequence of light absorption, electron-pairs are formed in the solid particle which can recombine or participate in reduction and oxidation reactions that result in the decomposition of contaminants. Halogenated and aromatic hydrocarbons, nitrogen-containing heterocyclic compounds, herbicides and many other compounds have been examined, particularly in water solution. Results have indicated that almost any organic and many of the inorganic pollutants produced by the electrical, electronic, agricultural, textile, petrochemical, metallurgical and many other industries can be completely destroyed or separated using a photocatalyst [2]. Research in this area, with particular emphasis in proving the feasibility of the concept, has produced a significant progress to the point that photocatalytic technologies are presently emerging in the marketplace. As it has frequently occurred in other fields, technological applications have been already developed, even though research has yet to succeed in providing a comprehensive understanding and description of the involved phenomena.

Thus, the development of a reliable knowledge basis is still in its initial stages since questions related to the chemistry and reaction networks of pollutant degradation, and problems posed by catalyst preparation, immobilization and photoactivation, catalyst chemical and mechanical stability, measurement of the optical properties of suspended particles and effects of irradiance levels constitute a combined challenge to find intrinsic kinetic rate data, the keystone to a sound photocatalytic reactor design [5].

This paper addresses some of the problems related to the second set of queries, using a fully irradiated annular heterogeneous photoreactor (FIP). Thus: (i) The impact of preparation procedures on suspensions' stability is evaluated, (ii) the optical properties of these suspensions are measured, (iii) special actinometric measurements are made in-situ to compute the incident radiation at the reactor boundaries, (iv) the RTE is solved for a very simple incident radiation model in order to evaluate, with a good degree of approximation, the LVREA inside the reactor volume and (v) the effects of relevant process variables (e.g., substrate, oxygen and catalyst concentration, LVREA) are determined to find intrinsic initial decomposition rates.

2. Experimental

A model titania photocatalyst (Aldrich, Cat. No 23,023-3: $S_g = 9.5$ m^2 g^{-1}; $d_p = 200$–300 nm; +99% anatase) and a priority pollutant (chloroform) were used throughout the work.

The experimental device (Fig. 1) was a multitube annular photoreactor (1) placed at one of the focal axes of a cylindrical reflector of elliptical cross section (2). A tubular, high pressure Hg vapor, 1200 W, UV lamp (Hanovia) (3) was placed in the second focal axis of the reflector. Recycling systems were driven by variable speed peristaltic pumps (Masterflex, Model 2650 MG) (4); the temperature was kept constant (25°C) using a thermostatic bath (MGW Lauda K4R) (5). The titania suspensions were maintained under magnetic stirring (6) in a closed Pyrex glass container with a total volume of 375 cm^3 (7).

The photoreactor consisted of a set of three concentric and coaxial Pyrex glass tubes; this arrangement served as a multi-purpose reactor/

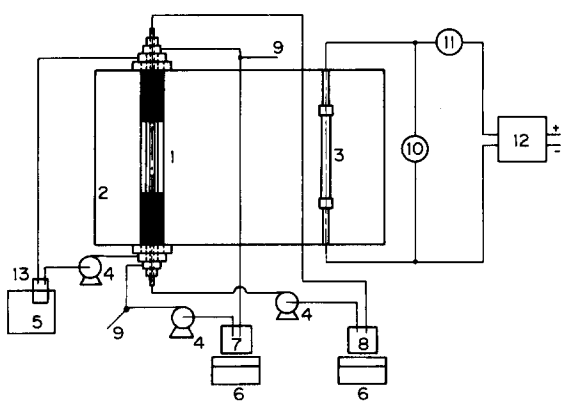

Fig. 1. Experimental device for the decomposition of chloroform. (1) photoreactor, (2) cylindrical reflector, (3) lamp, (4) peristaltic pumps, (5) thermostatic bath, (6) magnetic stirrer, (7) titania suspension, (8) actinometer, (9) thermometer, (10) voltmeter, (11) ammeter, (12) lamp source, (13) infrared filter.

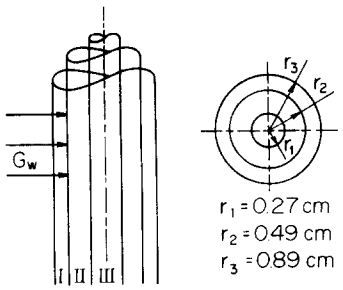

Fig. 2. Multitube annular photoreactor. (I) infrared filter, (II) reaction annulus, (III) inner tube. G_w, incident radiation at the wall (boundary condition).

measuring device (Fig. 2). The outer annulus I ($r_2 \rightarrow r_3$) acted both as an infrared filter (water, triply distilled and filtered with a 0.2 μm membrane) and as a thermostat; the intermediate annulus II ($r_1 \rightarrow r_2$) allowed first the actinometric measurement of the incident radiation at the reactor wall (boundary conditions G_w) and was used later for the photocatalytic degradation of chloroform. The inner tube III ($0 \rightarrow r_1$) was employed to quantify the radiation extinguished by the TiO_2 suspensions flowing through the intermediate annulus: FIP conditions (i.e., all the particles along the light path can 'see the photons') were achievable in the full range of TiO_2 concentrations that were used. Actinometric measurements were made with oxalic acid-uranil sulfate mixtures, following special procedures [6]. Degradation of chloroform was followed by gas chromatography (ECD; 1/8″–6 ft Porapak Q-S columns; isothermally at 180°C; carrier: N_2) with a head space technique in a Perkin-Elmer Sigma 2 unit. Homogeneous photolysis can be safely neglected because almost no radiation below 300 nm was present inside the reactor made of Pyrex glass.

Steady state operation was ensured prior to each run; three h were allowed to achieve reactor temperature and lamp operation stabilization. A mixture of oxygen and nitrogen (different concentrations according to experimental design) was bubbled into the suspensions (water plus catalyst, free of chloroform) for one h to make sure that saturation at specific conditions was reached. Chloroform was then added, in the desired amount, from a constant temperature saturated solution [7]. The whole system was tightly closed to prevent the formation of a gas phase in the reactor loop. The presence of a single, liquid phase was carefully controlled to make sure that no chloroform was escaping from the reacting solution.

The photocatalytic decomposition of $HCCl_3$ at room temperature was studied by varying the concentrations of (a) chloroform ($[HCCl_3] = 0$–100 μM), (b) dissolved oxygen ($[O_2] = 250$–1200 μM) and (c) titania ($W_c = 0.100$–0.200 kg m^{-3}), as well as (d) the intensity of the incident radiation, using calibrated screens (6, 29, 66 and 100% transmission). Table 1 details the experimental conditions for a total of 32 runs, as well as their grouping, to allow a parametric analysis of the results.

The powdered titania was dried overnight at 150°C in an oven prior to use. Water was 'pure', i.e., triply distilled, demineralized, free of organic content and filtered (0.2 μm membrane). The natural pH of the water (6.4) was not adjusted. Aqueous suspensions (0.030–0.200 kg m^{-3}) were prepared in 1000 cm^3 flasks, sonicated for 60 min. (Megason Model G-120-80-2) and allowed to stabilize for at least 48 h. Measurements of the apparent napierian extinctance (ANE) [8] of these suspensions (CARY 17DHC UV-vis-NIR spectrophotometer) showed long-term (5 days) stability across a wide range of frequencies (Fig. 3a). Furthermore, the different ANE values of the suspensions showed a linear dependence with the mass concentration of titania and with the length of the optical path, for all the wavelengths used in this work (see Fig. 3b for three wave-

Table 1
Experimental grid

Run nr.	W_c kg m^{-3}	$[O_2]$ μM	$[G_w/G_{max}]$	$[HCCl_3]$ μM
1–4	■	●	◆	90, 55, 29, 9
5–8	◧	●	◆	65, 46, 29, 22
9–12	□	●	◆	35, 30, 23, 15
13–16	■	◐	◆	80, 56, 24, 10
17–20	■	○	◆	84, 60, 25, 9
21–24	■	●	◈	86, 65, 27, 9
25–28	■	●	◈	91, 62, 29, 10
29–32	■	●	◇	86, 62, 38, 11

Experimental Grid. W_c: ■ 0.20, ◧ 0.15, □ 0.10 kg m^{-3}. $[O_2]$: ● 1200, ◐ 720, ○ 250 μM. $[G_w/G_{max}]$: ◆ 1, ◈ 0.66, ◈ 0.29, ◇ 0.06.

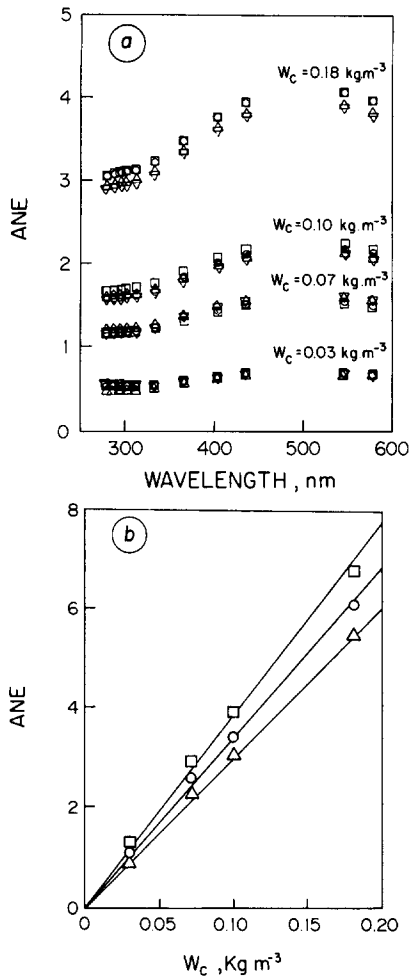

Fig. 3. (a) ANE of the titania suspensions vs. wavelength after ○: 0, □: 24, △: 96, ▽: 120 hours. (b) ANE of the suspensions vs. catalyst loading (W_c). Wavelengths: △ 302, ○ 366, □ 435 nm.

lengths). Therefore, a single optical parameter, the specific spectral apparent volumetric extinction coefficient (β^*), obtained from the experimental values of ANE, sufficed to characterize the said suspensions. Combined results from spectrophotometric and actinometric measurements showed that, within the range of solid concentrations and optical paths needed to sustain a FIP, a radial incidence radiation heterogeneous photoreactor model using solely the spectral specific volumetric extinction coefficient of the suspensions was enough to predict in a good first approximation the local volumetric rate of energy absorption (LVREA) in the inner tube (for a detailed discussion see Ref. [9]). Conversely, that under FIP conditions the knowledge of the optical properties of the suspension, extinction and absorption spectral specific volumetric coefficients (β^* and κ^*) [10], is required to evaluate the LVREA inside the annulus of reaction.

3. Results and discussion

3.1. Effects of the initial substrate concentration

Fig. 4a shows experimental data of the initial reaction rate of the chloroform decomposition, R_i, vs. initial substrate concentration, C_i, obtained with three different catalyst concentrations (0.100, 0.150 and 0.200 kg m^{-3}). They show that, within the range of process variables studied and under fully irradiated conditions, the reaction rate is of first order with respect to [$HCCl_3$]. Similar results (Fig. 4b) were observed when the boundary condition at the reactor wall (G_w) was changed, by using calibrated screens. For all the

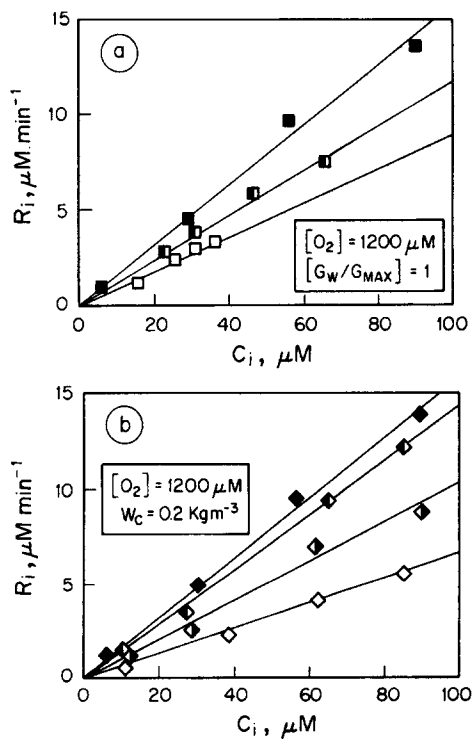

Fig. 4. Initial rate vs. initial chloroform concentration. (a) W_c: ■ 0.20, ◧ 0.15, □ 0.10 kg m^{-3}; (b) [G_w/G_{max}]: ◆ 1, ◈ 0.66, ◈ 0.29, ◇ 0.06. G_{max} = 12 μEinstein cm^{-2} min^{-1}.

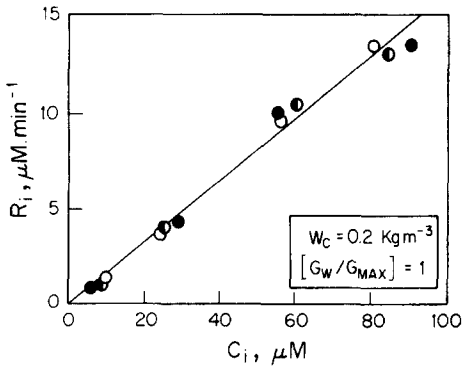

Fig. 5. Initial rate vs. initial chloroform concentration. [O_2]: ● 1200, ◐ 720, ○ 250 μM.

runs cited above, the oxygen concentration was kept constant (1200 μM).

3.2. Effects of the initial oxygen concentration

Fig. 5 shows the experimental initial reaction rate of the chloroform decomposition versus the initial concentration of substrate, obtained using several oxygen concentration conditions (runs 1–4 and 13–20). In this group of runs the concentration of titania ($W_c = 0.200$ kg m^{-3}) and the irradiation level ($[G_w/G_{max}] = 1$) were kept constant. These data show that, within the studied range of initial oxygen concentration ([O_2] = 250–1200 μM), the initial reaction rate was about equal (i.e., showed a zero order dependence with respect to [O_2]).

3.3. Effects of the LVREA

To determine a functional relationship between the measured reaction rate and the available incident radiation we need to evaluate the LVREA inside the reactor:

$$\text{LVREA} = e^a_\upsilon(r) = G_\upsilon(r)\,\kappa^*_\upsilon W_c \qquad (1)$$

where κ^*_υ is the specific volumetric absorption coefficient and G_υ is the incident radiation.

From the radiative transfer equation, using the radial incidence model [6] and with the hypothesis that in our experimental conditions the in-scattering is not significant [9], the following expression for the LVREA can be derived:

$$\text{LVREA} = e^a_\upsilon(r) = G_\upsilon(r)\,\kappa^*_\upsilon W_c = \kappa^*_\upsilon W_c \left\{ \frac{r_2}{r} G_{\upsilon,w} \exp[-\beta^*_\upsilon W_c (r_2 - r)] \right\} \qquad (2)$$

The LVREA is a function of position, frequencies, catalyst concentration and the boundary condition ($G_{\upsilon,w}$). The last one was evaluated by means of special actinometric measurements.

Although the LVREA is a spectral function which fully accounts for the absorption of radiative energy inside the reactor, we only need to consider those frequencies capable of exciting the catalyst ($\upsilon \geq \upsilon_0$), that is:

$$\text{LVREA}_T = \sum_{\upsilon \geq \upsilon_0} e^a_\upsilon \qquad (3)$$

$$\text{LVREA}_T = \sum_{\upsilon \geq \upsilon_0} e^a_\upsilon(r) = \sum_{\upsilon \geq \upsilon_0} G_\upsilon(r)\,\kappa^*_\upsilon W_c = \sum_{\upsilon \geq \upsilon_0} \kappa^*_\upsilon W_c \left\{ \frac{r_2}{r} G_{\upsilon,w} \exp[-\beta^*_\upsilon W_c (r_2 - r)] \right\} \qquad (4)$$

To avoid misinterpretation of the kinetic data we must recall that, very often, photoreactors operate under non uniform concentration, temperatures and radiation (light) distributions. In some cases good mixing can be achieved and non uniformities in concentrations and temperature may be minimized. However, by the proper nature of radiation propagation, a uniform distribution of photons inside the reactor can not be achieved. In other words, point (local) values of the reaction rates are not uniform and in many cases are utterly different from the overall (observable) ones; Eq. (4) clearly illustrates this point.

Fig. 6a shows the spatial variation of the LVREA_T as a function of the radial position according to Eq. (4) and within the annular reacting space (from $r_1 \leq r \leq r_2$). Numerical values correspond to the different titania concentrations employed in this work. From this representation it can be concluded that with these catalyst concentrations and this optical path length ($r_2 - r_1$) the photoreactor is always fully irradiated; i.e., always behaves as a FIP.

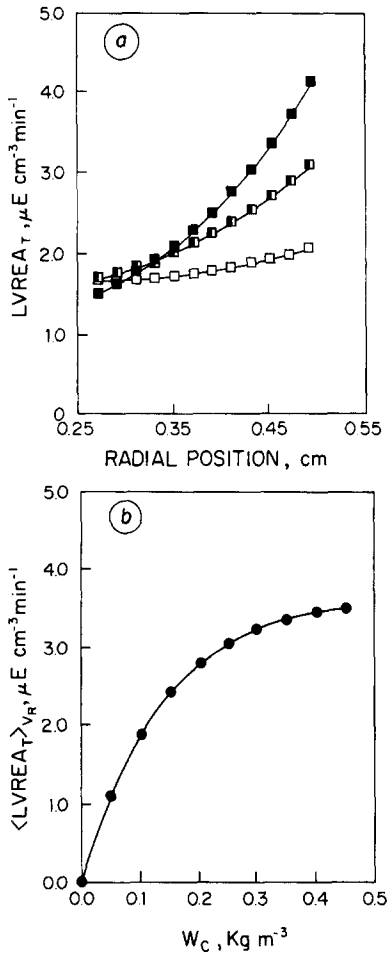

Fig. 6. (a) LVREA$_T$ distribution inside the photoreactor vs. radial coordinate. $r_1 = 0.27$, $r_2 = 0.49$ cm. W_c: ■ 0.20, ◧ 0.15, □ 0.10 kg m^{-3}. (b) ⟨LVREA$_T$⟩$_{V_R}$ vs. titania concentration (W_c), [G_w/G_{max}] = 1.

As it has been shown both theoretically [Eq. (4)] and experimentally (actinometry inside the inner tube) that the reactor is fully irradiated, all the catalyst particles are illuminated. An average over the whole reactor volume of LVREA$_T$ can be easily obtained by integration:

$$\left\langle \sum_{\upsilon \geq \upsilon_0} e_\upsilon^a \right\rangle_{V_R} = \langle \mathrm{LVREA_T} \rangle_{V_R}$$

$$= W_c \sum_{\upsilon \geq \upsilon_0} \frac{1}{V_R} \int_{V_R} \frac{r_2}{r} G_{\upsilon,w} \kappa_\upsilon^* \exp[-\beta_\upsilon^* W_c (r_2 - r)] \, dV \quad (5)$$

Fig. 6b represents the volume averaged values of the LVREA$_T$ as a function of the catalyst concentration. It can readily be seen that, in our device, the limiting condition of FIP (existence of 'dark regions' inside the reactor) can only be reached for catalyst loadings above 0.3 kg m^{-3}.

Based on the experimental evidence shown above, and assuming that the same reaction pathway is applicable throughout the FIP, the observable (i.e.: experimentally accessible) reaction rate, which is a volumetric average of local conditions, can be written as follows:

$$R_i = \langle f(W_c, C_i, \mathrm{LVREA_T}) \rangle_{V_R}$$

$$= C_i \langle \mathrm{LVREA}(W_c)_T^n \rangle_{V_R} \quad (6)$$

The volume-averaged values of the LVREA$_T$ was calculated for a set of experimental runs, using the full stock of calibrated screens and the same catalyst loading (runs 1–4, 21–32). Fig. 7 shows that the R_i/C_i ratio versus the ⟨LVREA$_T$⟩$_{V_R}$ follows a square root variation. Moreover, the experimental values agreed fairly well with the regression obtained by using a 0.5-order function for the ⟨LVREA$_T$⟩$_{V_R}$ (full line in Fig. 7).

Finally, with the complete set of experimental runs the following initial rate expression was obtained (with a variation coefficient, VC = 15.4%):

$$R_i = 0.0029 C_i \langle \mathrm{LVREA_T} \rangle_{V_R}^{0.5} \quad (7)$$

Further refinements showed that $\langle \mathrm{LVREA} \rangle^n \cong \langle \mathrm{LVREA}^n \rangle$ within ±3% for $0 \leq n \leq 2$ and $W_c \leq 0.2$ kg m^{-3}, so that for practical purposes the simpler expression:

$$R_i = 0.0029 C_i \langle \mathrm{LVREA_T^{0.5}} \rangle_{V_R} \quad (8)$$

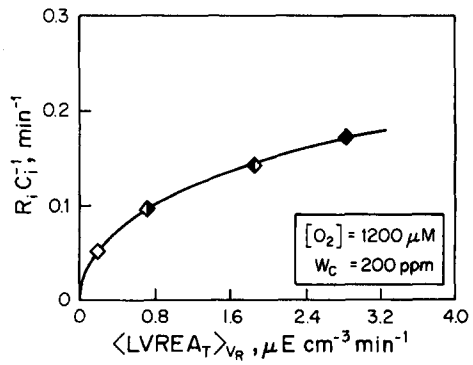

Fig. 7. Normalized chloroform decomposition (R_i/C_i) vs. ⟨LVREA$_T$⟩$_{V_R}$.

is equally suited.

This correlation coincides with a photocatalytic reaction scheme in which, at high enough irradiation conditions, the hole trapping by hydroxyl groups attached to surface Ti^{IV} atoms to form hydroxyl radicals (and/or the hole capture by the substrate itself) is the rate determining step (as the electron-hole recombination rate well exceeds the reaction rate). This reaction scheme is in accordance with results obtained by other research teams [11,12].

Summing up: The photocatalytic reaction rate is of first order with respect to $[HCCl_3]$, zero order with respect to $[O_2]$ and about one-half-order with respect to the $\langle LVREA_T \rangle$ inside the reactor. Secondly, the effects due to catalyst concentration are fully accounted for within the LVREA dependence. It may also be concluded that it is feasible to thoroughly evaluate reaction rates in photocatalytic processes using a fully irradiated photoreactor in which the LVREA is duly quantified for each situation.

4. Nomenclature

$C_i =$ Initial concentration of substrate, g mol m^{-3}, also μM.

$G_w =$ Incident radiation on the reactor wall, Einstein $m^{-2}\ s^{-1}$, also μE cm^{-2} min^{-1}.

$S_g =$ Specific surface area, $m^2\ g^{-1}$.

$W_c =$ Catalyst concentration, kg m^{-3}, also ppm.

$d_p =$ Particle diameter, m, also nm.

$e^a_\upsilon =$ Local volumetric rate of energy absorption, Einstein $m^{-3}\ s^{-1}$, also μE $cm^{-3}\ min^{-1}$.

$R_i =$ Initial reaction rate, g mol $m^{-3}\ s^{-1}$, also μM min^{-1}.

$r =$ Cylindrical coordinate, m, also cm.

$V_R =$ Reactor volume, m^{-3}, also cm^{-3}.

$\beta^*_\upsilon =$ Spectral specific volumetric extinction coefficient, $m^2\ kg^{-1}$.

$\upsilon =$ Radiation frequency, s^{-1}.

$\kappa^*_\upsilon =$ Spectral specific volumetric absorption coefficient, $m^2\ kg^{-1}$.

Acknowledgements

The authors are grateful to Consejo Nacional de Investigaciones Científicas y Técnicas (CONICET) and to Universidad Nacional del Litoral (U.N.L.) for their support to produce this work.

References

[1] M.A. Callahan and M. Slimak, N. Gbel, Report EPA-40014-74-029 a, b (1979).
[2] D.F. Ollis, E. Pelizzetti and N. Serpone, Environ. Sci. Technol., 25 (1991) 1523.
[3] R.W. Matthews, Water Res., 24 (1990) 653.
[4] D. Ollis and H. Al-Ekabi (Eds.), Photocatalytic Purification and Treatment of Water and Air, Elsevier, Amsterdam, 1993.
[5] National Research Council, Potential Applications of Concentrated Solar Photons, National Academy Press, Washington, 1991.
[6] A.E. Cassano, Revista de la Facultad de Ingeniería Química, 37 (1968) 469.
[7] C. Kormann, D.W. Bahnemann and M.R. Hoffmann, Environ. Sci. Technol., 25 (1991) 494.
[8] C.A. Martín, M.A. Baltanás and A.E. Cassano, J. Photochem. Photobiol. A: Chem., 76 (1993) 1991.
[9] C.A. Martín, Doctoral Thesis, Universidad Nacional del Litoral, Santa Fe, Argentina 1994.
[10] M.I. Cabrera, O.M. Alfano and A.E. Cassano, Ind. Eng. Chem. Res., 33 (1994) 3031.
[11] T.A. Egerton and C.J. King, J. Oil. Coll. Chem. Assoc., 62 (1979) 386.
[12] C.S. Turchi and D.F. Ollis, J. Catal., 122 (1990) 178.